



City Research Online

City, University of London Institutional Repository

Citation: Ma, H., Wang, Z., Wang, L., Zhang, Q., Yang, Z. & Bao, Y. (2016). Ramp heating in high-speed transient thermal measurement with reduced uncertainty. *Journal of Propulsion and Power*, 32(5), pp. 1190-1198. doi: 10.2514/1.b35803

This is the accepted version of the paper.

This version of the publication may differ from the final published version.

Permanent repository link: <https://openaccess.city.ac.uk/id/eprint/15542/>

Link to published version: <https://doi.org/10.2514/1.b35803>

Copyright: City Research Online aims to make research outputs of City, University of London available to a wider audience. Copyright and Moral Rights remain with the author(s) and/or copyright holders. URLs from City Research Online may be freely distributed and linked to.

Reuse: Copies of full items can be used for personal research or study, educational, or not-for-profit purposes without prior permission or charge. Provided that the authors, title and full bibliographic details are credited, a hyperlink and/or URL is given for the original metadata page and the content is not changed in any way.

City Research Online:

<http://openaccess.city.ac.uk/>

publications@city.ac.uk

Ramp Heating in High-Speed Transient Thermal Measurement with Reduced Uncertainty

H. Ma,* Z. Wang,* L. Wang,* and Q. Zhang†

Shanghai Jiao Tong University, 200240 Shanghai, People's Republic of China

and

Z. Yang and Y. Bao

AVIC Commercial Aircraft Engine Company, Ltd., XXXXXX Shanghai, People's Republic of China

DOI: 10.2514/1.B35803

The uncertainty associated with the convective heat transfer coefficient obtained in transient thermal measurement is often high, especially in high-speed flow. The present study demonstrates that the experimental accuracy could be much improved by an actively controlled ramp heating instead of the conventional step-heating approach. A general design guideline for the proposed ramp-heating method is derived theoretically and further demonstrated by simulation cases. This paper also presents a detailed experimental study for transonic turbine blade-tip heat transfer. A repeatable, high-resolution tip heat transfer coefficient contour is obtained through transient infrared measurement with the proposed ramp-heating method. Detailed uncertainty analysis shows that the resulting heat transfer coefficient uncertainty level is much lower than the experimental data currently available in the open literature. The ramp-heating approach is especially recommended to the high-speed heat transfer experimental research community to improve the accuracy of the transient thermal measurement technique.

Nomenclature

C_x	=	axial chord, m
c	=	specific heat, J/kg · K
D	=	noise distribution
f	=	sampling frequency, Hz
G	=	grayscale value
h	=	heat transfer coefficient, W/(m ² · K)
k_{avg}	=	average slope
M	=	Mach number
N	=	number of simulation test
np	=	number of sampling points
P_0	=	mainstream total pressure, Pa
q''	=	heat flux, W/m ²
Re	=	Reynolds number
R^2	=	coefficient of determination
r_c	=	recovery factor
T_{ad}	=	adiabatic wall temperature, K
T_i	=	initial temperature, K
T_w	=	wall temperature, K
T_0	=	mainstream total temperature, K
t	=	time, s
U	=	uncertainty
x	=	horizontal axis of sampled signal
y	=	vertical axis of sampled signal
γ	=	ratio of specific heats
Δ	=	overall change during selected interval
δ	=	noise level
λ	=	thermal conductivity, W/(m · K)
ρ	=	density, kg/m ³
τ	=	time constant, s

I. Introduction

Gas turbine heat transfer technology has reached, more or less, a plateau in recent years. The improvements from new thermal designs are usually small. A designer will not be able to rank their design ideas from an experimental study if the uncertainty level is in the range of 10%. Unfortunately, such an uncertainty level is not uncommon among the heat transfer experimental data currently available in the open literature. Very often, the computational fluid dynamics developers find it difficult to rank their turbulence models and other new numerical methods with the available experimental data if taking the experimental uncertainty into account. Improving the uncertainty in conventional experimental techniques is particularly required by the heat transfer research community.

Transient thermal measurement techniques have been widely employed in various heat transfer experimental studies. One common assumption made in these techniques is the semi-infinite one-dimensional conduction, which means conduction within solid occurs only in one direction toward infinity. This is a fair assumption if the heat penetration depth is small when compared with the actual thickness of the solid. Therefore, a low-conductivity material is often used in experiments to satisfy this assumption. Another classical assumption is that the mainstream temperature experiences an ideal step change at time origin. This perfect step is, undeniably, impossible to achieve in practice, but tremendous efforts have been devoted to creating a mainstream temperature step change as sharp as possible so that this second assumption can be justified approximately (Ireland [1], Martinez-Botas et al. [2], Gillespie et al. [3], and Ireland et al. [4]). Under these two assumptions, the wall temperature history $T_w(t)$ is then readily obtained as (Bergman et al. [5])

$$\frac{T_w(t) - T_i}{T_0 - T_i} = 1 - \exp\left(\frac{h^2 t}{\rho c \lambda}\right) \operatorname{erfc}\left(\frac{h \sqrt{t}}{\sqrt{\rho c \lambda}}\right) \quad (1)$$

where T_0 is the mainstream total temperature, T_i is the initial temperature, h is the heat transfer coefficient (HTC), and λ is the thermal conductivity of fluid. In practice, when the mainstream temperature is a ramp varying profile, the resulting wall temperature history can be calculated from Duhamel's superposition theorem (Metzger and Larson [6]):

Received 14 March 2015; revision received 4 January 2016; accepted for publication 8 April 2016; published online XX epubMonth XXXX. Copyright © 2016 by the American Institute of Aeronautics and Astronautics, Inc. All rights reserved. Copies of this paper may be made for personal and internal use, on condition that the copier pay the per-copy fee to the Copyright Clearance Center (CCC). All requests for copying and permission to reprint should be submitted to CCC at www.copyright.com; employ the ISSN 0748-4658 (print) or 1533-3876 (online) to initiate your request.

*University of Michigan–Shanghai Jiao Tong University Joint Institute.

†University of Michigan–Shanghai Jiao Tong University Joint Institute City; currently University of London, London, England, U.K.; Qiang.Zhang@City.ac.UK (Corresponding Author).

$$T_w(t) - T_i = \sum_{j=1}^N \left\{ \left[1 - \exp\left(\frac{h^2(t - \tau_j)}{\rho c \lambda}\right) \cdot \operatorname{erfc}\left(\frac{h\sqrt{t - \tau_j}}{\sqrt{\rho c \lambda}}\right) \right] \cdot (\Delta T_o)_j \right\} \quad (2)$$

Therefore, once the wall temperature history is measured, the HTC can be calculated from Eq. (1) for the step heating and Eq. (2) for the ramp heating, respectively.

The wall transient thermal responses can be discretely recorded by thermocouples, resistance temperature detectors, and thin-film gauges. To capture the spatial variations at a higher resolution, optical measurement techniques, such as thermochromic liquid crystal (TLC) and infrared (IR) thermography, are broadly applied. TLC coated on the test surface will reflect different colors if the surface temperature alters. This distinctive property leads to the wide application of the TLC technique in transient thermal measurement. Metzger et al. [7] sprayed TLC coatings on a rotating surface and observed their response during the transient measurement, which was then processed to calculate the surface HTC. The experimental uncertainty was estimated to be $\pm 10\%$ in their study. Ekkad and Han [8] developed image-processing techniques for TLC measurement in a series of turbine blade internal cooling and film-cooling thermal measurements. The uncertainty of the HTC in their study ranged from ± 4.8 to $\pm 6.5\%$. A similar procedure with a single narrowband TLC was employed by Chanteloup et al. [9]. They investigated the heat transfer distribution in a two-pass internal coolant passage and reported an uncertainty in the HTC of approximately $\pm 8\%$. Teng et al. [10] obtained an uncertainty level of $\pm 8.3\%$ for HTC distributions on a large-scale gas turbine blade tip. A detailed uncertainty analysis for TLC transient thermal measurement was carried out by Yan and Owen [11]. Their analysis was in good agreement with computed values obtained using a Monte Carlo method. It was shown how the experimental uncertainty could be minimized by a proper selection of the temperature range of the TLC. IR thermography detects surface radiation energy and quantifies the surface temperature. It has several advantages, such as its nonintrusiveness, high sensitivity (down to 20 mK), fast response time (down to 20 μ s), and wide temperature range (-20 to 1500°C), as summarized by Carlomagno and Cardone [12]. Schulz [13] introduced an in situ calibration procedure to convert an IR camera's raw data into temperature readings with high accuracy. Ekkad et al. [14,15] solved the HTC and film-cooling effectiveness simultaneously from one single transient thermal test by recording temperature distributions at two different instants with an IR camera of 60 Hz. The run-to-run error of performing two different tests to obtain two unknowns (HTC and film-cooling effectiveness) was avoided, and the uncertainty in the derived HTC and film-cooling effectiveness was $\pm 4.5\%$ and $\pm 7.0\%$.

During transient thermal measurement, it is worth noting that there should be a huge time difference in the wall temperature response for a low-conductivity testing material under high and low HTC values in the mainstream. Such a different time response will either bring up different requirements for instrumentations and sensing techniques or introduce different levels of experimental errors. Figure 1 demonstrates the typical wall temperature responses to a step change of the mainstream total temperature for HTC values of 100 and 2000 $\text{W}/(\text{m}^2 \cdot \text{K})$. They are calculated from Eq. (1) by assuming a step increase of 20 K in the mainstream total temperature, with a $\sqrt{\rho c \lambda}$ value of 600 $\text{J}/\text{m}^2 \cdot \text{K} \cdot \text{s}^{0.5}$ (typical of Perspex material). Here, a time constant τ is defined as the time required to reach 63.2% of the total temperature change. Figure 1 indicates that a 20-times increase in the HTC value results in 400-times reduction in the time constant τ (56 s versus 0.14 s). In the real experimental practice dealing with high HTCs, the wall temperature trace within the first 0.14 s has to be well captured in order to accurately reduce HTC data from Eq. (1) or Eq. (2), which implies a much more demanding requirement for the sampling frequency of the data acquisition (DAQ) system to be employed.

It is not uncommon to have HTC values over 2000 $\text{W}/(\text{m}^2 \cdot \text{K})$, especially in high-speed heat transfer experiments. Mee et al. [16]

reported a $\pm 15\%$ uncertainty level in Stanton number distribution on a flat-plate surface in a supersonic flow. This high uncertainty level was mainly caused by the large error in capturing the rapid TLC color change in the short-duration tunnel. Zhang et al. [17,18] and O'Dowd et al. [19] measured turbine blade-tip heat transfer under transonic conditions ($M_{\text{exit}} = 1.0$). A step change in the mainstream temperature was generated by a heater mesh, and the blade-tip surface temperature response was recorded by an IR camera of 60 Hz. The HTC value for each tip point was derived by linear regression between the heat flux and surface temperature history during a selected period of heating. The blade-tip HTC contour ranged from 800 to 2000 $\text{W}/(\text{m}^2 \cdot \text{K})$, with an average uncertainty of $\pm 9.5\%$. The uncertainty level associated with high HTCs must be much higher than 10% due to the inadequacy of the IR camera's sampling frequency (to capture the fast transient process after the step heating). On the other hand, the regions with high HTC values are of particular interest to engine designers and researchers. It has been recognized that reducing the experimental uncertainty in high HTC values (especially high-speed flow) is still a big challenge.

The demands for capturing a fast temperature response within a short period after step heating can be easily reduced by a controlled ramp-heating method. As illustrated in Fig. 2, the mainstream temperature is controlled to increase linearly instead of having a step change. Hence, the transient thermal period is effectively extended and more surface temperature data can be collected for the HTC derivations. Potentially, this approach will reduce the experimental uncertainty in transient thermal measurements, especially in high-speed flow. There have been some existing studies using ramp heating in transient thermal measurement: for instance, Mee et al. [16], Roy et al. [20], and Anto et al. [21]. However, the intentions of these works were not on uncertainty reduction. A systematic analysis of reducing the experimental uncertainty by controlling the ramp-heating method is lacking in the open literature.

The present study investigates a controlled ramp-heating concept to reduce the experimental uncertainty in the HTC in high-speed IR transient heat transfer experiments. The paper begins with a detailed analysis regarding the relationships between the uncertainty level, the ramp slope, the sampling frequency, and the HTC. A general design

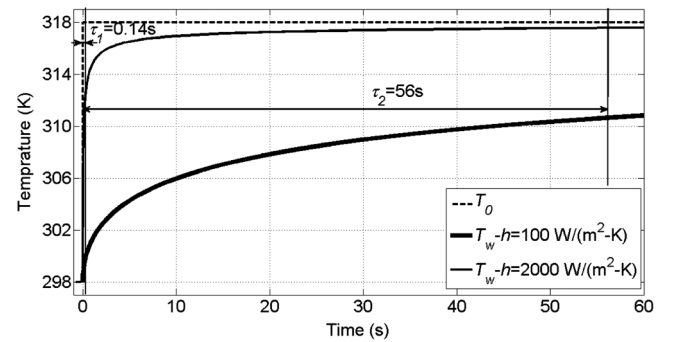


Fig. 1 Wall temperature responses to a step change of the mainstream total temperature for high and low HTC values.

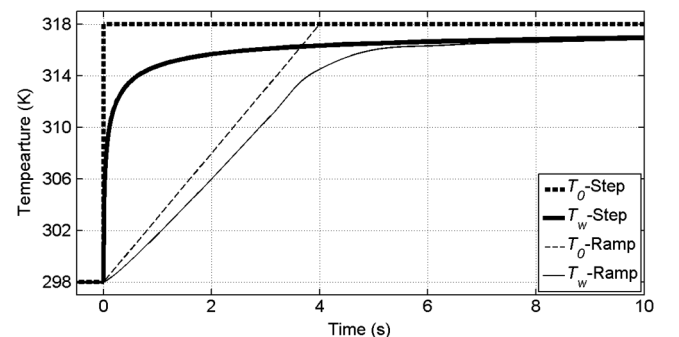


Fig. 2 Wall temperature response to step and ramp changes in the mainstream temperature, for $\text{HTC} = 2,000 \text{ W}/(\text{m}^2 \cdot \text{K})$.

guideline for the ramp-heating transient experiments is then derived and demonstrated by numerical cases. The second half of the paper implements the ramp-heating concept into an experimental study for transonic turbine blade-tip heat transfer. The performance of ramp heating in a high-speed wind-tunnel experiment is demonstrated through spatially resolved HTC results with reduced measurement uncertainty and compared with the conventional step-heating approach.

II. Error Analysis for Controlled Ramp Heating

In experiments, the object quantity (such as the HTC) can be calculated based on the sampled measurement data (for example, temperature). For any sampled signal, in a prescribed timespan between (x_1, y_1) and (x_2, y_2) , the average slope k_{avg} is

$$k_{\text{avg}} = \frac{\int_{x_1}^{x_2} (dy/dx) dx}{x_2 - x_1} \quad (3)$$

Because of the known dependent relations [e.g., Eq. (1) or Eq. (2)] from theory or analysis, the accuracy of this slope determines the accuracy of the objective quantities.

Suppose the measurement is repeated N times, from each of which $k_{\text{avg},i}$ ($i = 1, \dots, N$) can be obtained. The mean of these $k_{\text{avg},i}$ is

$$\overline{k_{\text{avg}}} = \frac{1}{N} \sum_{i=1}^N k_{\text{avg},i} \cdot \text{RMSE}(k_{\text{avg}})$$

The root-mean-square error (RMSE) of the average slope

$$\left(\sqrt{\frac{1}{N} \sum_{i=1}^N (k_{\text{avg},i} - \overline{k_{\text{avg}}})^2} \right)$$

then defines the relative error (RE) of the measurement:

$$RE_{k_{\text{avg}}} = \frac{\text{RMSE}(k_{\text{avg}})}{\overline{k_{\text{avg}}}} \times 100\% \quad (4)$$

In principle, for any $y(x)$, $RE_{k_{\text{avg}}}$ depends on the following parameters: the number of sampling points np , the noise distribution D , and the relative noise level $(\delta y/y_2 - y_1)$, where δy is the noise level of each sampling point. Typically, the noise distribution D and δy are functionally determined by the instrument. For a specified sampling frequency f , the number of sampling points np is related with k_{avg} as

$$np = \frac{(y_2 - y_1) \cdot f}{k_{\text{avg}}} \quad (5)$$

The influences from np and $\delta y/y_2 - y_1$ on $RE_{k_{\text{avg}}}$ need to be independent in principle. From the law of large numbers in statistics, the convergence of the root-mean-square error is proportional to the number of sampling points np . In addition, $RE_{k_{\text{avg}}}$ should be linearly dependent on the relative noise level $(\delta y/y_2 - y_1)$. It then yields

$$RE_{k_{\text{avg}}} = c_1 \cdot \frac{\delta y}{y_2 - y_1} \cdot \sqrt{\frac{k_{\text{avg}}}{(y_2 - y_1) \cdot f}} \quad (6)$$

The preceding discussion only deals with the relative error of k_{avg} . The relative error RE_h of the target parameter HTC is related to $RE_{k_{\text{avg}}}$ by the following formula:

$$RE_h = RE_{k_{\text{avg}}} \cdot p_{\text{fit}}(k_{\text{avg}} \rightarrow h) \quad (7)$$

where $p_{\text{fit}}(k_{\text{avg}} \rightarrow h)$ is the dimensionless propagation factor from $RE_{k_{\text{avg}}}$ to RE_h , which needs to be determined analytically from case to case. Altogether, the error analysis here consists of two steps: first,

to calculate the relative error of the sampled signal; and second, to obtain the relative error of the target parameter by multiplying with the propagation factor.

In the following, a case study of a high-speed heat transfer experiment is presented for detailed illustration.

Experimentally, what we can obtain from measurement is the wall temperature history $T_w(t)$. For the proposed ramp-heating method, the target parameter HTC can be calculated by data fitting through Eq. (2) via all the sampled points between $(t_1, T_w(t_1))$ and $(t_2, T_w(t_2))$. The noise level δT_w is prescribed by temperature sensor calibration, accuracy of the DAQ system, etc. The maximum temperature rise is the overall temperature change during the selected interval $[\Delta T_w = T_w(t_2) - T_w(t_1)]$. Then, Eq. (6) is reduced to

$$RE_{k_{\text{avg}}} = c_2 \cdot \sqrt{\frac{k_{\text{avg}}}{\Delta T_w \cdot f}} \quad (8)$$

For the propagation factor from k_{avg} to h , the ramp-heating solution Eq. (2) indicates

$$p_{\text{fit}}(k_{\text{avg}} \rightarrow h) \approx \frac{c_3}{\sqrt{k_{\text{avg}}}} + c_4 \quad (9)$$

where c_3 and c_4 are constants (detailed derivation in the Appendix). The relative error of the HTC can then be expressed as

$$RE_h = \frac{c_5}{\sqrt{f}} + c_6 \sqrt{\frac{k_{\text{avg}}}{f}} \quad (10)$$

where the constants c_5 and c_6 are HTC dependent. For $\text{HTC} = 2000 \text{ W}/(\text{m}^2 \cdot \text{K})$, $c_5 = 0.216 \text{ s}^{-0.5}$ and $c_6 = 0.0348 \text{ K}^{-0.5}$ based on the simulation test results. Equation (10) suggests two ways to reduce the relative error of the HTC. One is to increase f by employing a DAQ system with a higher sampling frequency; the other is to reduce k_{avg} by heating up the mainstream with a slower rate.

The preceding analysis [e.g., Eq. (10)] is a new approach to understand how the experimental inaccuracy will be influenced (via sampling rate, ramp-heat rate, and HTC value) and how it can be estimated or predicted in a quantitative manner, which can be meaningful in experiment assessment and design as a general guideline.

To quantify the relative error of the HTC, MATLAB simulation tests were implemented by changing the inputs as follows.

Let the mainstream temperature vary in three different slopes for a HTC value of $2000 \text{ W}/(\text{m}^2 \cdot \text{K})$, as shown in Fig. 3a. The resulting wall temperature responses with three average slopes are then calculated from Eq. (2), as shown in Fig. 3b. The time interval used for data fitting is determined by constant $\Delta T_w = 10 \text{ K}$. The wall temperature responses of the three average slopes are all approximately linear. The noise level δT_w is set to be $\pm 1.0 \text{ K}$. All of these inputs are summarized in Table 1. It should be noted that, for the first case, the T_0 slope is very large, which can be approximately regarded as the conventional step heating under real scenarios.

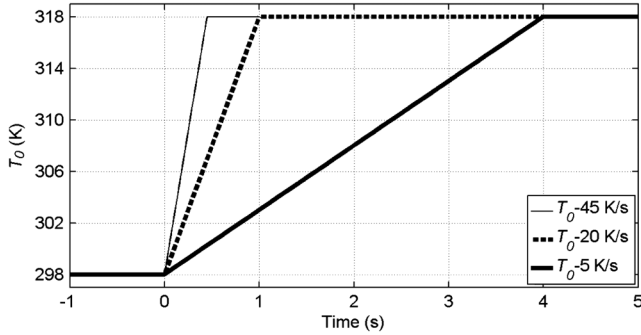
The simulation is implemented via the following steps:

- 1) Choose one case and solve $T_w(t)$ by Eq. (2).
- 2) Choose a numerical sampling frequency f and disturb T_w at each sampled point by the random noise δT_w . Then, substitute it back into Eq. (2) to obtain the HTC value after data fitting h_{fit} .
- 3) Repeat step 2 N times to obtain $h_{\text{fit},i}$, $i = 1, 2, \dots, N$ for the estimation of the relative error of the HTC.

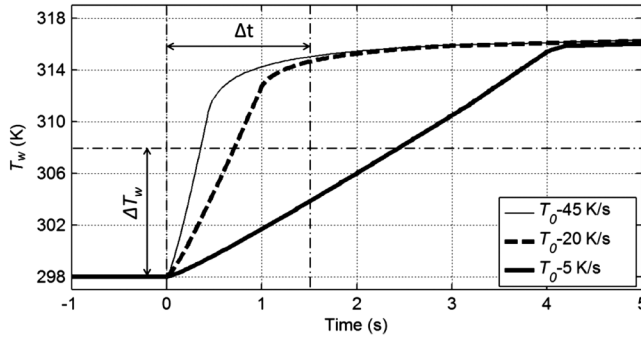
Here, the number of simulation test N is 10,000 so that the obtained results are statistically meaningful. For each simulation test, the fitting error ε_i is

$$\varepsilon_i = h_{\text{fit},i} - h_{\text{true}} \quad (11)$$

From N simulation tests,



a) Mainstream temperature



b) Wall temperature response

Fig. 3 Temperature histories of three ramp-heating methods [HTC = 2000 W/(m² · K)].

$$\text{RMSE}(h) = \sqrt{\frac{1}{N} \sum_{i=1}^N \varepsilon_i^2}$$

Then, the relative error of HTC, i.e.,

$$\text{RE}_h = \frac{\text{RMSE}(h)}{h_{\text{true}}} \times 100\%$$

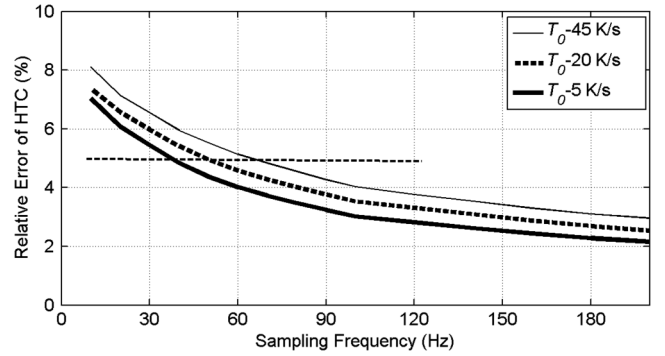
can be calculated. For different cases, the dependences of the relative error of the HTC on the sampling frequency are summarized in Fig. 4. As expected, for each set of wall temperature signals, the relative error of the HTC decreases rapidly as the sampling frequency increases. If set an acceptable relative error level, e.g., 5% (shown by the dashed line), there is a much more stringent requirement for sampling frequency in the near-step-heating case than that for the ramp case. On the other hand, if we set a fixed sampling frequency, the HTC relative error is larger for the wall temperature signal with a bigger slope. Table 2 summarizes the simulation test results for three cases. It is shown that, to achieve the same level of accuracy,

$$\text{RE}_h = 5\%, \quad \frac{c_5}{\sqrt{f}} + c_6 \sqrt{\frac{k_{\text{avg}}}{f}}$$

is a constant, which nicely proves Eq. (10).

Figure 5 demonstrates the relative errors at different HTC values for both the step and the ramp-heating method from the simulation test results, at a fixed sampling frequency of 30 Hz (typical of an ordinary IR camera) and a same wall temperature change ΔT_w of

	Case number		
	1	2	3
T_0 slope, K/s	45	20	5
Time interval for data fitting, s	0–0.36	0–0.72	0–2.46
T_w average slope k_{avg} , K/s	28.73	14.45	4.18

Fig. 4 Relative error of the HTC as a function of sampling frequencies [HTC = 2000 W/(m² · K)].

10 K. When the HTC value is lower than 500 W/(m² · K), both the step-heating method and the ramp-heating method can achieve good accuracy (less than 2%). However, as the HTC value increases from 1000 to 3000 W/(m² · K) (typical in transonic and supersonic flows), the uncertainty level of the ramp-heating method can be reduced up to 50%.

However, it should be noted that the ramp-heating method also has its limitations in practice. Within a fixed transient period Δt , the increase in wall temperature from the ramp-heating method can be much lower than the step-heating case, especially for low HTC values. In these cases, the ratio of the noise level δT_w to the increase in wall temperature ΔT_w from initial conditions can play an important role in the overall uncertainty [see Eq. (6)]. The advantage of the ramp-heating method is manifested only if the HTC value is high or the transient period Δt is long enough. For further understanding of the tradeoff situation, Fig. 6 demonstrates a contour of ratios of uncertainty levels between two heating methods (at a sampling frequency of 30 Hz). Clearly, the ramp-heating method can only provide better performance than the step-heating method in the region of high HTC values or a longer transient period. Therefore, it is not recommended to apply the ramp-heating method in the short-duration thermal experiments with low HTC values.

III. Transient IR Thermal Measurement for a Transonic Turbine Blade Tip

In this part, the ramp-heating method proposed previously is applied in transient IR thermal measurement for a transonic turbine blade-tip heat transfer study. Detailed experimental approaches and the results with uncertainty analysis are described.

A. Experimental Setup

A transonic blowdown wind tunnel was employed to conduct the transient heat transfer experiment in the present study, as shown in Fig. 7. Compressed air with a maximum pressure of 3 MPa was contained in a 10 m³ air storage tank. A Fisher control valve (EWT body with 667 actuator and Fieldvue DVC6000 controller) regulated the total pressure at the inlet of the test section in the testing plenum. An extended Karman-filter-based control algorithm was developed to predictively adjust the valve opening (Xi et al. [22]). Honeycomb screens and flow straighteners were located downstream of the

Table 2 Summary of simulation test results

	Case number		
	1	2	3
Frequency-5% ^a f_5 , Hz	70	50	30
δT_w , K	±1.0		
$c_5/\sqrt{f} + c_6\sqrt{k_{\text{avg}}/f}$	0.050 ± 0.002		

^aFrequency-5% signifies sampling frequency required to achieve 5% relative error of the HTC.

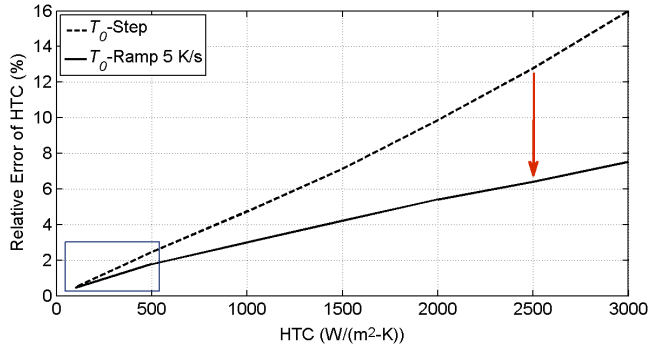


Fig. 5 Relative error at different HTC values for step- and ramp-heating methods (sampling frequency: 30 Hz, $\Delta T_w = 10$ K).

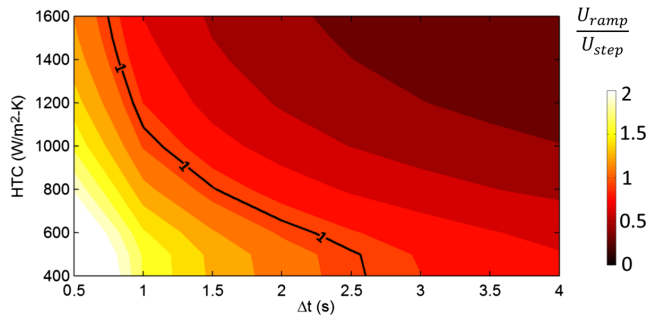


Fig. 6 Ratios of uncertainty levels between the ramp- (5 K/s) and step-heating methods at various transient periods.

control valve to ensure the flow quality. A heater mesh was installed before the testing plenum to heat up the mainstream flow during the heat transfer experiment. This heater mesh was connected to a 100 kW dc power supply. The actual output of the power supply could be remotely programmed and controlled by the DAQ system and a

customized LabVIEW program. As a result, the mainstream temperature could be manipulated to be a step or a ramp (or any other profiles). The test section was located inside a testing plenum, which could also hold various other test sections. The exhaust pipeline also had a regulating valve so the pressure of the testing plenum could be adjusted. More details for the flow characteristic and wind-tunnel design were described in work by Evans et al. [23] and Chen [24].

Figure 8 shows the details of the test section and instrumentations. The linear cascade consists of seven blades and six passages to achieve the periodicity of the flowfield. There are also two boundary-layer bleeds on two sidewalls. The blade has an axial chord C_x of 0.039 m and is scaled from a certain high-pressure turbine blade design condition. For the three blades in the middle of the cascade, the upper parts are made from resin with low thermal conductivity by stereolithography technology and the lower parts are made from steel for fixing purposes. In the present study, the tip gap height is approximately 1% of the blade span. A FLIR A325 researcher IR camera with a spatial resolution of 320×240 is installed right above the central blade of the linear cascade, and in between is a zinc-selenide (ZnSe) IR window. The IR camera records the tip surface temperature history at a frequency of 60 Hz during a blowdown run. One thermocouple is placed on the tip surface to perform in situ calibration of the camera (instead of relying on the camera’s built-in calibration). Such a practice is to minimize the uncertainties introduced by surface emissivity, IR window transmissivity, radiation from surroundings, etc. Figure 9 shows an example of the linear calibration relation between the image grayscale values and the temperature readings from a surface thermocouple.

The inlet total temperature was measured by a thermocouple (K type, Omega) probe mounted upstream of the test section, for which the wire diameter was 0.076 mm (0.003 in.) and the response time was less than 80 ms. It was sampled at 80 Hz by a National Instruments PXIe DAQ system and interpolated to match the IR frequency.

Flow conditions for the transonic turbine blade-tip heat transfer experiment are summarized in Table 3. Detailed time histories of the inlet mainstream total pressure and total temperature are illustrated in Fig. 10. The flow is stabilized 5 s after the opening of the control valve

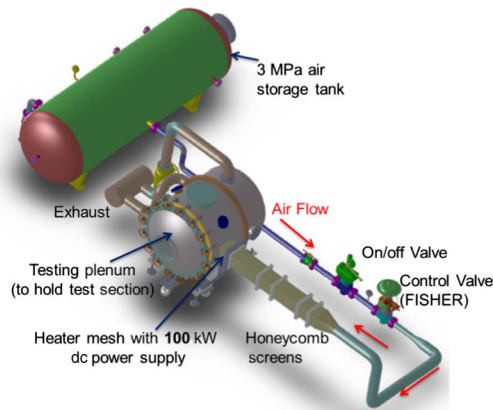


Fig. 7 Transonic wind-tunnel facility in the present study.

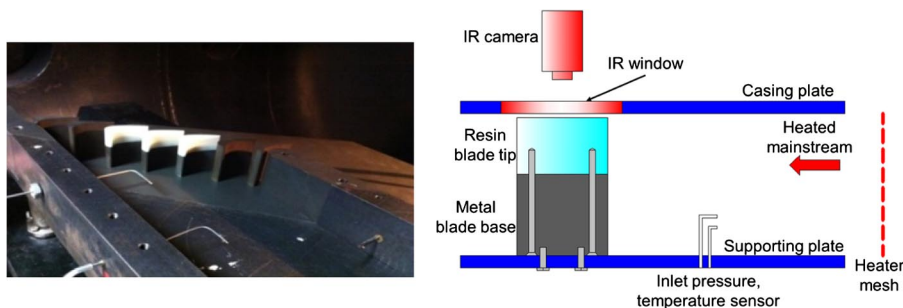


Fig. 8 Test section employed in the present study.

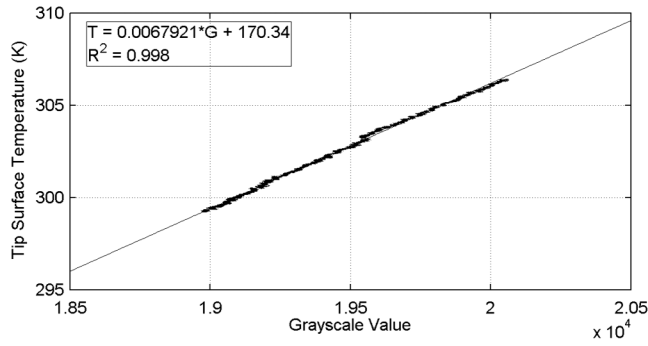


Fig. 9 IR camera calibration curve.

and the heater mesh is turned on right afterward. In the present study, the T_w signal is sampled at 60 Hz by the IR camera. The maximum mainstream temperature rise is limited to be 20 K due to the heating power (100 kW). According to the error analysis in Sec. II (Fig. 4), a slower surface temperature response (smaller k_{avg}) will be preferred to minimize the HTC uncertainty. By linearly controlling the heating power, the mainstream total temperature increases at a rate of 5 K/s, as shown in Fig. 10. Three seconds of the transient thermal measurement data during the ramp heating are selected to calculate the surface HTC values. For comparison purpose, the step-heating method is applied as well, and its resulting mainstream total temperature history is also shown in Fig. 10.

B. Data Reduction Method

In the present study, the HTC is defined according to the Newton's law of cooling:

$$q'' = h(T_{ad} - T_w) \quad (12)$$

where q'' is the heat flux, T_w is the wall temperature, and T_{ad} is the adiabatic wall temperature that can be expressed as

$$T_{ad} = \frac{1 + r_c(\gamma - 1/2)M^2}{1 + (\gamma - 1/2)M^2} T_0 = c_{ad}(M, r_c, \gamma) \Delta T_0 \quad (13)$$

In this equation, T_0 is the mainstream total temperature, M is the Mach number of the mainstream, γ is the ratio of specific heats of the fluid, and r_c is the recovery factor (which can be approximated to be a function of Prandtl number). Once the flowfield reaches a steady state, the coefficient c_{ad} will be a specific constant for a surface location, i.e., T_{ad} will be proportional to T_0 .

Take Eq. (13) into Eq. (12) and rearrange:

$$\frac{q''}{T_0} = -h \frac{T_w}{T_0} + hc_{ad} \quad (14)$$

From the transient temperature history, q'' can be reconstructed using the impulse method by Oldfield [25]. This method has been employed in a series of previous studies (Zhang et al. [17,18] and O'Dowd et al. [26]) and proved to be accurate, computationally efficient, and reliable. To account for the preheating before the turning on of the mesh heater, the complete surface temperature data from the start of the blowdown run were used to reconstruct the heat

Table 3 Flow conditions for the present experimental study

Parameter	Value
Inlet total pressure, Pa	180,000
Inlet Mach number	0.3
Inlet Reynolds number (based on C_x)	0.26×10^6
Exit static pressure, Pa	101,325
Exit Mach number	0.95
Exit Reynolds number (based on C_x)	0.88×10^6
Mass flow rate, kg/s	3

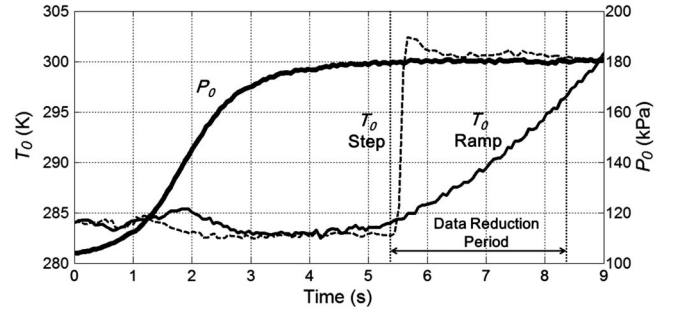


Fig. 10 Time histories of the inlet mainstream total pressure and mainstream total temperature.

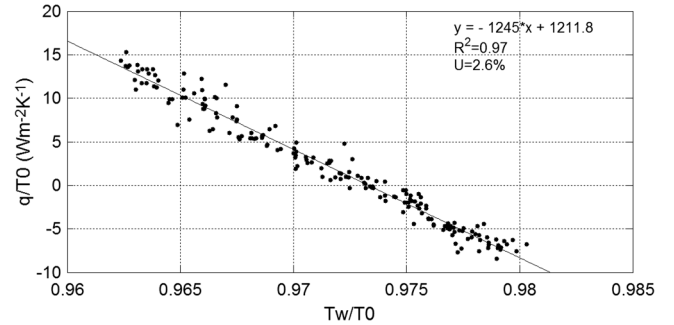


Fig. 11 Regression line for one selected point on the tip surface.

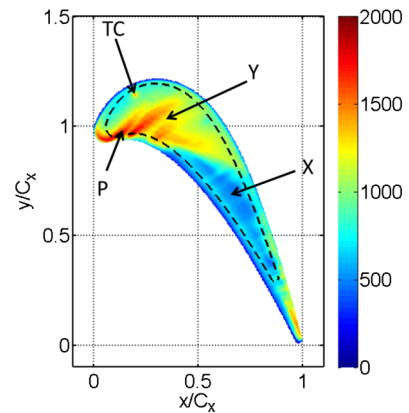


Fig. 12 Contour of HTC for the transonic turbine blade tip [$W/(m^2 \cdot K)$] (lateral conduction error is negligible within the dashed curve).

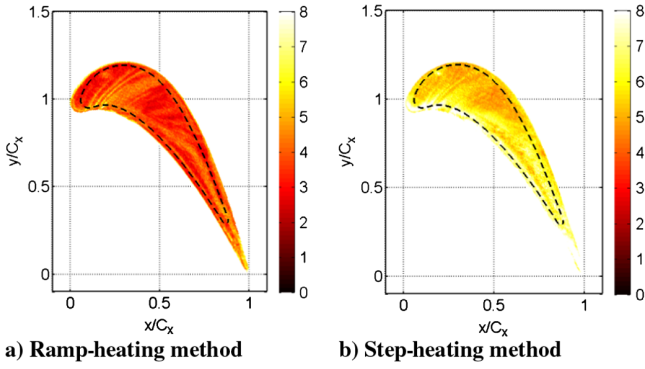
flux history. Next, h and c_{ad} could be obtained from linear regression of q''/T_0 and T_w/T_0 for every blade-tip location. According to Eq. (14), preheating did not change the slope of the regression line. It only offset the coefficient c_{ad} .

Note that, potentially, the regression error could be very large if not enough "effective" wall temperature data could be obtained in the experiments. In the conventional step-heating approach, the errors from the regression process directly resulted in poor repeatability and large overall uncertainty level, especially for the high HTCs.

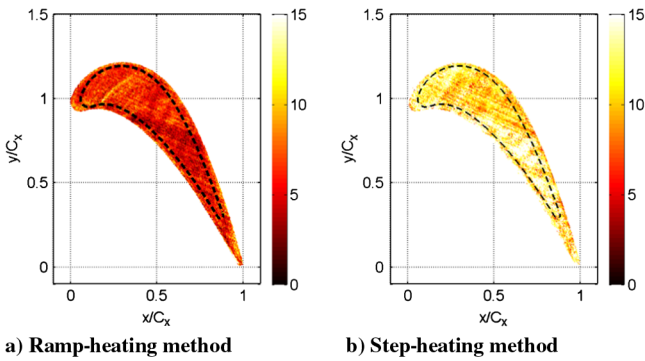
Figure 11 illustrates the performance of regression from the proposed ramp-heating method. The temperature trace was obtained for a selected point on the midchord of the blade-tip surface. All data points (T_w/T_0 , q''/T_0) were evenly scattered around the regression line. The coefficient of determination R^2 in statistics (Devore [27]) was 0.97. The relative uncertainty in linear regression was 2.6% with 95% confidence (Coleman and Steele [28]). Such linear regression performance was very satisfactory and highly repeatable. For this selected point, the slope of regression line indicated $h = 1245 W/(m^2 \cdot K)$.

C. Tip HTC Contour and Uncertainty Improvement

Figure 12 shows a sample of the tip HTC contour obtained with the ramp-heating approach. Around the sharp edge of the tip surface,



a) Ramp-heating method b) Step-heating method
Fig. 13 Contour of relative uncertainty in linear regression (in percentages).



a) Ramp-heating method b) Step-heating method
Fig. 14 Contours of relative uncertainty in HTC (in percentages) obtained from four repeated experiments.

16 lateral conduction becomes a major source of experimental error. According to Chen et al. [29], the one-dimensional semi-infinite conduction assumption can introduce over a 20% error near the corner region. Such an error can be effectively reduced by a correction technique proposed by Chen et al. [29]. A corner conduction error is not corrected in the present study, since the main focus here is to address the improvement in experimental uncertainty by ramp heating. A dashed line is determined based on the penetration depth analysis, as shown in Fig. 12. Within 3 s of transient heating, this line is roughly 1.3 mm away from the tip edge for the ramp heating and will be 1.8 mm for the step heating. Only the HTC data within the enclosed region are discussed next. The HTC results from different heating approaches are compared with the same transient heating period (3 s).

17 The overall pattern of the HTC contour shown in Fig. 12 agrees quite well with tip heat transfer results recently published by Zhang et al. [17,18]. In leading-edge portion of blade (region Y) HTC is well over $1200 \text{ W}/(\text{m}^2 \cdot \text{K})$. Peak values of the HTC occur near the leading-edge stagnation point (region P), which have the range of 1500 to $1800 \text{ W}/(\text{m}^2 \cdot \text{K})$. The HTC is considerably lower [below $600 \text{ W}/(\text{m}^2 \cdot \text{K})$] in rear region X than the frontal part of the blade. A small spot of the high HTC in the leading edge (region TC) relates to the interference from the thermocouple placed on the tip surface for IR camera calibration.

Figure 13a shows the relative uncertainty (95% confidence) in linear regression for each data point on the tip surface. The relative uncertainty in the linear regression is below 5% within the dashed curve of the blade tip. For the purpose of comparison, a transient IR

measurement using the conventional step-heating approach is also carried out. The obtained distribution of the HTC is the same as that derived by the ramp-heating method, as illustrated in Fig. 12. But, its uncertainty level is much higher, as shown in Fig. 13b. For most areas within the dashed curve of the blade tip, the relative uncertainty in the linear regression is above 5%. The high uncertainty areas on the blade tip may also be attributed to flow unsteadiness associated with the local vortical flow structure or shock-wave/boundary-layer interactions (Zhang et al. [17,18]). These additional sources of local measurement noises have not been considered in the previous analytical approach.

Finally, four repeated experiments are conducted to examine the consistency of the results. The obtained contours of the relative uncertainty in the HTC with 95% confidence are presented in Fig. 14a for the ramp-heating method and in Fig. 14b for the step-heating method. These uncertainties are generated not only from the linear regression error during each test but also from the run-to-run error between different tests. For the ramp-heating method, the relative uncertainty in the HTC is below 8% for the entire blade-tip surface, whereas for the step-heating method, the value is 15%. Thus, experimental uncertainty can be reduced 50% by applying the proposed ramp-heating method.

Overall measurement uncertainties for the present study are summarized in Table 4. With results from multiple runs, the relative uncertainty of area-averaged HTC is $\pm 6.1\%$. Compared with the uncertainty level of around $\pm 9.5\%$ in similar high-speed experiments by Zhang et al. [17,18] and Anto et al. [21], there is a remarkable improvement with the proposed ramp-heating method.

IV. Conclusions

The uncertainty associated with the conventional transient thermal measurement technique and an improved approach by ramp heating has been investigated in the present study.

The theoretical analysis indicates that actively controlling the mainstream temperature ramp in transient measurement has remarkable advantages over the conventional step heating. Although the HTC values are high, the solid surface temperature has a fast response (time constant less than 1 s for typical low-conductivity material). It has been demonstrated that the demanding requirements for acquiring the temperature response and minimizing the measurement error can be eased by ramp heating. A new approach was developed to understand how the experimental inaccuracy will be influenced (via sampling rate, wall temperature response, and HTC value) and how it can be predicted in a quantitative manner, which is useful in experiment assessment and design as a general guideline.

The improvement in experimental accuracy with a controlled ramp-heating approach in high-speed flows has been further demonstrated in a transonic turbine blade-tip heat transfer study. A high-resolution tip HTC contour was obtained through transient IR thermal measurement in a transonic linear cascade facility (exit Mach number M_{exit} of 0.95 and exit Reynolds number Re_{exit} of 0.88×10^6). A detailed uncertainty analysis showed that the linear regression uncertainty in deriving HTC values from one single experiment with the ramp-heating method was much lower than that obtained by the step-heating method.

In conclusion, the present study demonstrates that the controlled ramp-heating approach could provide an additional useful degree of freedom for optimizing the experimental accuracy in transient thermal measurement, and it is especially recommended to the high-speed experimental heat transfer community.

Appendix A: Derivation of the Propagation Factor

Denote the difference between the wall temperature and the initial temperature as

$$T_d(t) = T_w(t) - T_i = (T_0 - T_i) \left[1 - \exp\left(\frac{h^2 t}{\rho c \lambda}\right) \operatorname{erfc}\left(\frac{h \sqrt{t}}{\sqrt{\rho c \lambda}}\right) \right] \quad (\text{A1})$$

Table 4 Measurement uncertainties

Measurement	Relative uncertainty 95% confidence
Wall temperature T_w	0.4 ($300 \pm 1.2 \text{ K}$)
Mainstream total temperature T_0	0.4 ($300 \pm 1.2 \text{ K}$)
Area-averaged HTC	6.1 [$909.74 \pm 55.49 \text{ W}/(\text{m}^2 \cdot \text{K})$]

The random noise in T_d will result in fluctuations of the HTC derived by backsubstitution of Eq. (1). To quantify their relationship, the following equation is derived:

$$\begin{aligned} \frac{RE_h}{RE_{T_d}} &= \frac{\delta h/h}{\delta T_d/T_d} \approx \frac{\partial h}{\partial T_d} \frac{T_d}{h} = \frac{1}{\partial T_d/\partial h} \frac{T_d}{h} \\ &= \frac{1 - \exp(h^2 t/\rho c \lambda) \operatorname{erfc}(h\sqrt{t}/\sqrt{\rho c \lambda})}{\exp(h^2 t/\rho c \lambda) \operatorname{erfc}(h\sqrt{t}/\sqrt{\rho c \lambda}) 2h^2 t/\rho c \lambda - 2/\sqrt{\pi}(h\sqrt{t}/\sqrt{\rho c \lambda})} \\ &= g_p \left(\frac{h\sqrt{t}}{\sqrt{\rho c \lambda}} \right) \end{aligned} \quad (\text{A2})$$

In the ramp-heating method, the mainstream temperature is controlled to increase linearly with time, as shown in Fig. 3; then, the resulting wall temperature history $T_w(t)$ follows Eq. (2) and is close to a linear profile during the transient thermal process selected, as shown in Fig. 4. Thus,

$$\frac{\delta T_d}{T_d} \approx \frac{\delta k_{\text{avg}}}{k_{\text{avg}}}$$

and

$$t \approx \frac{\Delta T_w}{k_{\text{avg}}}$$

For a particular high-speed heat transfer experiment, h and ΔT_w are fixed; the propagation factor is then calculated as

$$\begin{aligned} p_{\text{fit}}(k_{\text{avg}} \rightarrow h) &= \frac{RE_h}{RE_{k_{\text{avg}}}} = \frac{\delta h/h}{\delta k_{\text{avg}}/k_{\text{avg}}} \approx \frac{\delta h/h}{\delta T_d/T_d} \\ &\approx g_p \left(\frac{h}{\sqrt{\rho c \lambda}} \sqrt{\frac{\Delta T_w}{k_{\text{avg}}}} \right) = g_p \left(\frac{c_{a1}}{\sqrt{k_{\text{avg}}}} \right) \end{aligned} \quad (\text{A3})$$

Here, c_{a1} is a constant. The form of the function g_p is determined from the simulation test results as Eq. (9).

Acknowledgments

The authors would like to acknowledge Aeronautical Scientific Funding for their financial support. The authors would also thank Li He from the University of Oxford for his insightful suggestions and advice.

References

- [1] Ireland, P., "Internal Cooling of Turbine Blades," Ph.D. Dissertation, Univ. of Oxford, Oxford, England, U.K., 1987.
- [2] Martinez-Botas, R., Lock, G., and Jones, T., "Heat Transfer Measurements in an Annular Cascade of Transonic Gas Turbine Blades Using the Transient Liquid Crystal Technique," *Journal of Turbomachinery*, Vol. 117, No. 3, 1995, pp. 425–431.
- [3] Gillespie, D., Wang, Z., and Ireland, P., "Heating Element," British Patent Application PCT/GB96/2017, 1995.
- [4] Ireland, P., Neely, A., Gillespie, D., and Robertson, A., "Turbulent Heat Transfer Measurements Using Liquid Crystals," *International Journal of Heat and Fluid Flow*, Vol. 20, No. 4, 1999, pp. 355–367.
- [5] Bergman, T., Lavine, A., Incropera, F., and DeWitt, D., *Fundamentals of Heat and Mass Transfer*, Wiley, New York, 2011.
- [6] Metzger, D., and Larson, D., "Use of Melting Point Surface Coatings for Local Convection Heat Transfer Measurements in Rectangular Channel Flows with 90-Deg Turns," *Journal of Heat Transfer*, Vol. 108, No. 1, 1986, pp. 48–54.
- [7] Metzger, D., Bunker, R., and Bosch, G., "Transient Liquid Crystal Measurement of Local Heat Transfer on a Rotating Disk with Jet Impingement," *Journal of Turbomachinery*, Vol. 113, No. 1, 1991, pp. 52–59.
- [8] Ekkad, S. V., and Han, J.-C., "A Transient Liquid Crystal Thermography Technique for Gas Turbine Heat Transfer Measurements," *Measurement Science and Technology*, Vol. 11, No. 7, 2000, pp. 957–968.
- [9] Chanteloup, D., Juaneda, Y., and Bolcs, A., "Combined 3-D Flow and Heat Transfer Measurements in a 2-Pass Internal Coolant Passage of Gas Turbine Airfoils," *Journal of Turbomachinery*, Vol. 124, No. 4, 2002,

pp. 710–718.

doi:10.1115/1.1506176

- [10] Teng, S., Han, J. C., and Azad, G. M. S., "Detailed Heat Transfer Coefficient Distributions on a Large-Scale Gas Turbine Blade Tip," *Journal of Heat Transfer*, Vol. 123, No. 4, 2001, pp. 803–809. doi:10.1115/1.1373655
- [11] Yan, Y. Y., and Owen, J. M., "Uncertainties in Transient Heat Transfer Measurements with Liquid Crystal," *International Journal of Heat and Fluid Flow*, Vol. 23, No. 1, 2002, pp. 29–35. doi:10.1016/s0142-727x(01)00125-4
- [12] Carlomagno, G. M., and Cardone, G., "Infrared Thermography for Convective Heat Transfer Measurements," *Experiments in Fluids*, Vol. 49, No. 6, 2010, pp. 1187–1218.
- [13] Schulz, A., "Infrared Thermography as Applied to Film Cooling of Gas Turbine Components," *Measurement Science and Technology*, Vol. 11, No. 7, 2000, pp. 948–956. doi:10.1088/0957-0233/11/7/311
- [14] Ekkad, S. V., Ou, S. C., and Rivir, R. B., "A Transient Infrared Thermography Method for Simultaneous Film Cooling Effectiveness and Heat Transfer Coefficient Measurements From a Single Test," *Journal of Turbomachinery*, Vol. 126, No. 4, 2004, pp. 597–603. doi:10.1115/1.1791283
- [15] Ekkad, S. V., Ou, S. C., and Rivir, R. B., "Effect of Jet Pulsation and Duty Cycle on Film Cooling From a Single Jet on a Leading Edge Model," *Journal of Turbomachinery*, Vol. 128, No. 3, 2006, pp. 564–571. doi:10.1115/1.2185122
- [16] Mee, D. J., Chiu, H. S., and Ireland, P. T., "Techniques for Detailed Heat Transfer Measurements in Cold Supersonic Blowdown Tunnels Using Thermochromic Liquid Crystals," *International Journal of Heat and Mass Transfer*, Vol. 45, No. 16, 2002, pp. 3287–3297. doi:10.1016/s0017-9310(02)00050-9
- [17] Zhang, Q., He, L., Wheeler, A., Ligrani, P., and Cheong, B., "Overtip Shock Wave Structure and Its Impact on Turbine Blade Tip Heat Transfer," *Journal of Turbomachinery*, Vol. 133, No. 4, 2011, Paper 041001.
- [18] Zhang, Q., O'Dowd, D., He, L., Oldfield, M., and Ligrani, P., "Transonic Turbine Blade Tip Aerothermal Performance with Different Tip Gaps—Part I: Tip Heat Transfer," *Journal of Turbomachinery*, Vol. 133, No. 4, 2011, Paper 041027.
- [19] O'Dowd, D. O., Zhang, Q., He, L., Oldfield, M. L. G., Ligrani, P. M., Cheong, B. C. Y., and Tibbott, I., "Aerothermal Performance of a Winglet at Engine Representative Mach and Reynolds Numbers," *Journal of Turbomachinery*, Vol. 133, No. 4, 2011, Paper 041026. doi:10.1115/1.4003055
- [20] Roy, A., Jain, S., Ekkad, S. V., Ng, W. F., Lohaus, A. S., and Crawford, M. E., "Heat Transfer Performance of a Transonic Turbine Blade Passage in Presence of Leakage Flow Through Upstream Slot and Mateface Gap With Endwall Contouring," ASME International Paper GT2014-26476, Fairfield, NJ, 2014.
- [21] Anto, K., Xue, S., Ng, W., Zhang, L., and Moon, H., "Effects of Tip Clearance Gap and Exit Mach Number on Turbine Blade Tip and Near-Tip Heat Transfer," ASME International Paper GT2013-94345, Fairfield, NJ, 2013.
- [22] Xi, J., Zhang, Q., Li, M., and Wang, Z., "Advanced Flow Control for Supersonic Blowdown Wind Tunnel Using Extended Kalman Filter," ASME International Paper GT2013-95281, Fairfield, NJ, 2013.
- [23] Evans, R., Dawes, W., and Zhang, Q., "Application of Design of Experiment to a Gas Turbine Cascade Test Cell," ASME International Paper GT2013-94314, Fairfield, NJ, 2013.
- [24] Chen, W., "Improvements on Conventional Transient Thermal Measurement on Turbine Blade," M.S. Thesis, Shanghai Jiao Tong Univ., Shanghai, PRC, 2013.
- [25] Oldfield, M. L. G., "Impulse Response Processing of Transient Heat Transfer Gauge Signals," *Journal of Turbomachinery*, Vol. 130, No. 2, 2008, pp. 1–9. doi:10.1115/1.2752188
- [26] O'Dowd, D. O., Zhang, Q., He, L., Ligrani, P. M., and Friedrichs, S., "Comparison of Heat Transfer Measurement Techniques on a Transonic Turbine Blade Tip," *Journal of Turbomachinery*, Vol. 133, No. 2, 2011, Paper 021028. doi:10.1115/1.4001236
- [27] Chen, W., Jiang, H., Zhang, Q., and He, L., "A Simple Corner Correction Technique for Transient Thermal Measurement," ASME International Paper GT2014-26622, Fairfield, NJ, 2014.
- [28] Moore, J., *Probability and Statistics for Engineering and the Sciences*, Engage Learning, 2011.
- [29] Rastogi, R. K., Man, H. W., and Steele, W. G., *Experimentation, Validation, and Uncertainty Analysis for Engineers*, Wiley, New York, 2009.

Queries

1. AU: Please check that the copyright (©) type is correct. Please note that the code will be added upon publication 
2. AU: The mailing code has been added for Shanghai Jiao Tong University. Please confirm it is correct 
3. AU: Only one affiliation can appear under each author's name. Please choose among these approaches for Zhang: A) It is customary to list the affiliation at the time of writing at the top, and a subsequent affiliation can be listed in the footnote. For this approach, please indicate which affiliation was at the time of writing and which is current. B) If preferred, only the current affiliation can be listed at the top. For this approach, please indicate the former affiliation and it will be removed. C) If the author currently has a double affiliation, please indicate which one is the primary and should appear at the top. Option A is shown in the current proof. 
4. AU: As AIAA prefers that each author have an affiliation footnote, please provide information for Yang and Bao. This may include job title, department, street address, email address, and/or AIAA membership 
5. AU: Please provide the mailing codes for AVIC Commercial Aircraft Engine Company, Ltd. and the University of London 
6. AU: Definitions of acronyms and abbreviations have been moved from the abstract into the text of the article, per AIAA style. 
7. AU: As AIAA reserves the Nomenclature for only defining variables, definitions of acronyms and/or terms have been moved from the nomenclature into the text of the article, per AIAA style. 
8. AU: CFD has been defined as computational fluid dynamics. Please confirm this is correct. 
9. AU: Please note that AIAA requires acronyms be used more than once to remain in the paper. 
10. AU: The sentence beginning "If set an acceptable relative..." is unclear/incomplete. Please review and edit as necessary 
11. AU: Instructions from AIAA indicate that figures are to appear in color only online. Please verify the usage of color in your proof is correct, and note that all figures will be grayscale in the print journal. 
12. AU: Please define EW 
13. AU: Please confirm that "Karman filter" is correct and should not be changed to "Kalman filter". 
14. AU: Header rows have been added to some of the tables, per journal guidelines. Please confirm your meaning was retained. 
15. AU: The text reads "Devore [27]," but Ref. [27] is by Chen et al. Please review and edit as necessary.
16. AU: The text reads "Chen et al. [29]," but Ref. [29] is by Coleman and Steele. Please review and edit as necessary.
17. AU: The text reads "Chen et al. [29]," but Ref. [29] is by Coleman and Steele. Please review and edit as necessary 
18. AU: As AIAA requires all units of measure be spelled out when not preceded by a number, please write out $W/(m^2 \cdot K)$ 
19. AU: The sentence beginning "In leading-edge portion of blade..." is unclear/incomplete. Please review and edit as necessary. 
20. AU: Please note that AIAA requires the final section be titled "Conclusions" 

21. AU: Please provide the pages used for Refs. [5, 29] 

22. AU: For Ref. [28], please provide the location of the publisher and the pages used 